PALAIOS
Emphasizing the impact of life on Earth's history

PALAIOS, 2025, v. 40, 131–140
Research Article
DOI: 10.2110/palo.2024.027

RIBBON-LIKE COMPRESSION FOSSILS FROM THE LATE EDIACARAN ESMERALDA MEMBER OF THE DEEP SPRING FORMATION AT MOUNT DUNFEE, NEVADA, USA

MARY C. LONSDALE,[1] KELSEY R. MOORE,[1] LUCY C. WEBB,[1,2] MIA SCHILDBACH,[3] KENNETH J.T. LIVI,[1,4] AND EMILY F. SMITH[1]
[1]*Department of Earth and Planetary Sciences, Johns Hopkins University, Baltimore, Maryland 21218, USA*
[2]*Earth and Planetary Sciences, Stanford University, 450 Jane Stanford Way, Stanford, California 94305 USA*
[3]*Baltimore Polytechnic Institute, 1400 W Cold Spring Lane, Baltimore, Maryland 21209, USA*
[4]*Materials Characterization and Processing, 800 Wyman Park Dr., Johns Hopkins University, Baltimore, Maryland 21211, USA*
email: mlonsdale@jhu.edu

ABSTRACT: We describe > 200 ribbon-like macroscopic fossils from terminal Ediacaran strata at Mount Dunfee, Nevada, USA ~ 115 m below the local placement of the Ediacaran–Cambrian boundary. They are preserved as casts and molds, composed of Fe-oxides and Fe-rich aluminosilicates in an aluminosilicate clay matrix. Measurements of 50 of the specimens provide a fossil size range of 0.22–0.74 mm-wide and 0.1–75.0 mm-long. Some specimens evidence original flexibility and appear to be fragmented, consistent with soft body preservation. They are therefore interpreted as body fossils, rather than trace fossils. Given this interpretation, we suggest that the fossils' size range and ribbon-like morphologies are consistent with them being members of the problematicum *Vendotaenia*, which have not been previously reported from Ediacaran strata within the southern Great Basin. The phylogenetic affinity of vendotaenids is unresolved, but they are commonly interpreted as a form of eukaryotic macroalgae. This report firmly establishes vendotaenids in Ediacaran strata on Laurentia, broadening their known paleogeographic range during the end-Ediacaran Period. Additionally, the morphology of the fossils described here supports the notion that, although vendotaenids are reported from many Ediacaran paleocontinents globally, there was low macroalgal diversity at the end of the Ediacaran Period.

INTRODUCTION

Two extinction events are hypothesized to have occurred in the terminal Ediacaran Period as a result of environmental catastrophe and/or biotic replacement (e.g., Kimura et al. 1997; Laflamme et al. 2013; Darroch et al. 2015, 2018, 2023; Wood et al. 2019). These extinction events are argued from biodiversity trends interpreted from the Ediacaran fossil record of complex soft-bodied macrobiota, with the first interpreted from an apparent abrupt drop in morphological diversity c. 550 Ma (Muscente et al. 2019; Evans et al. 2022; Darroch et al. 2023; Bowyer et al. 2024), and the second interpreted from fossil disappearances in strata ≤ 538 Ma (Knoll and Carroll 1999; Amthor et al. 2003; Hodgin et al. 2021; Smith et al. 2023; Bowyer et al. 2024). The fossil record of macroscopic eukaryotic algae (macroalgae) also hints at a terminal Ediacaran extinction event(s); time-binned carbonaceous compression macroalgal fossils reveal a decrease in morphospace range, morphological disparity, functional-form groups, maximum dimension, and alpha diversity at ~ 550–539 Ma (Bykova et al. 2020).

Confident interpretation of the evolutionary history of macroalgae is critical to understanding Ediacaran ecosystem dynamics. Before the appearance of seagrasses in the Mesozoic, macroalgae were the only eukaryotic primary producers within the marine biome (Aires et al. 2011). As such, they may have played an outsized role in driving biogeochemical change during the Paleozoic, Neoproterozoic, and Mesoproterozoic eras (LoDuca et al. 2017). Additionally, some Ediacaran macroalgae are suggested to have formed microhabitats, resulting in niche construction (Bykova et al. 2020), an important ecological function of modern coastal seaweeds (e.g., Levin 1991; Christie et al. 2009). Building regional and global Ediacaran macroalgal fossil records is, therefore, necessary to gain a more complete picture of terminal Ediacaran ecosystems and ecological change. However, due to the relatively low sampling intensity of terminal Ediacaran algal fossil assemblages, as well as a paucity of precise age constraints on them, apparent trends in macroalgal diversity across the terminal Ediacaran Period are not definitive (Xiao and Dong 2006; Bykova et al. 2020). Spatial variation in macroalgal trends is poorly constrained for the same reason; it is not clear how the composition of Ediacaran macroalgal communities changed over time, or whether changes to these communities were similar, globally.

Over the past few decades, investigation of terminal Ediacaran strata from the southern Great Basin has resulted in the discovery of numerous body fossil assemblages spanning a range of taphonomic modes (Hagadorn and Waggoner 2000; Hagadorn et al. 2000; Rowland and Rodriguez 2014; Smith et al. 2016, 2017, 2023; Selly et al. 2020). These fossil assemblages include vermiform fauna and problematic smooth-walled tubular fossils preserved as pyrite pseudomorphs, three-dimensional casts and molds, and compressed casts and molds (Smith et al. 2016, 2017, 2023; Hagadorn and Waggoner 2000; Selly et al. 2020; Rivas et al. 2024). They also include soft-bodied discoidal fossils and erniettomorphs (Smith et al. 2016, 2017; Hagadorn and Waggoner 2000; Hagadorn et al. 2000) and a branching alga (*Elainabella deepspringensis*) preserved as a carbonaceous compression (Rowland and Rodriguez 2014). Aside from these reports, no tubiform or ribbon-like algal fossils have yet been reported from Ediacaran strata in this region. This is despite the dominance of tubiform or ribbon-like algal morphotypes in terminal Ediacaran algal assemblages globally (Bykova et al. 2020), as well as the regional presence of nonalgal aluminosilicate casts and molds, a taphonomic mode from which tubiform or ribbon-like algae (*Grypania* and *Vendotaenia*) are sometimes reported (e.g., Han and Runnegar 1992; Kumar 1995; Cohen et al. 2009). Here, we contribute to the regional

Published Online: May 2025
 0883-1351/25/040-131

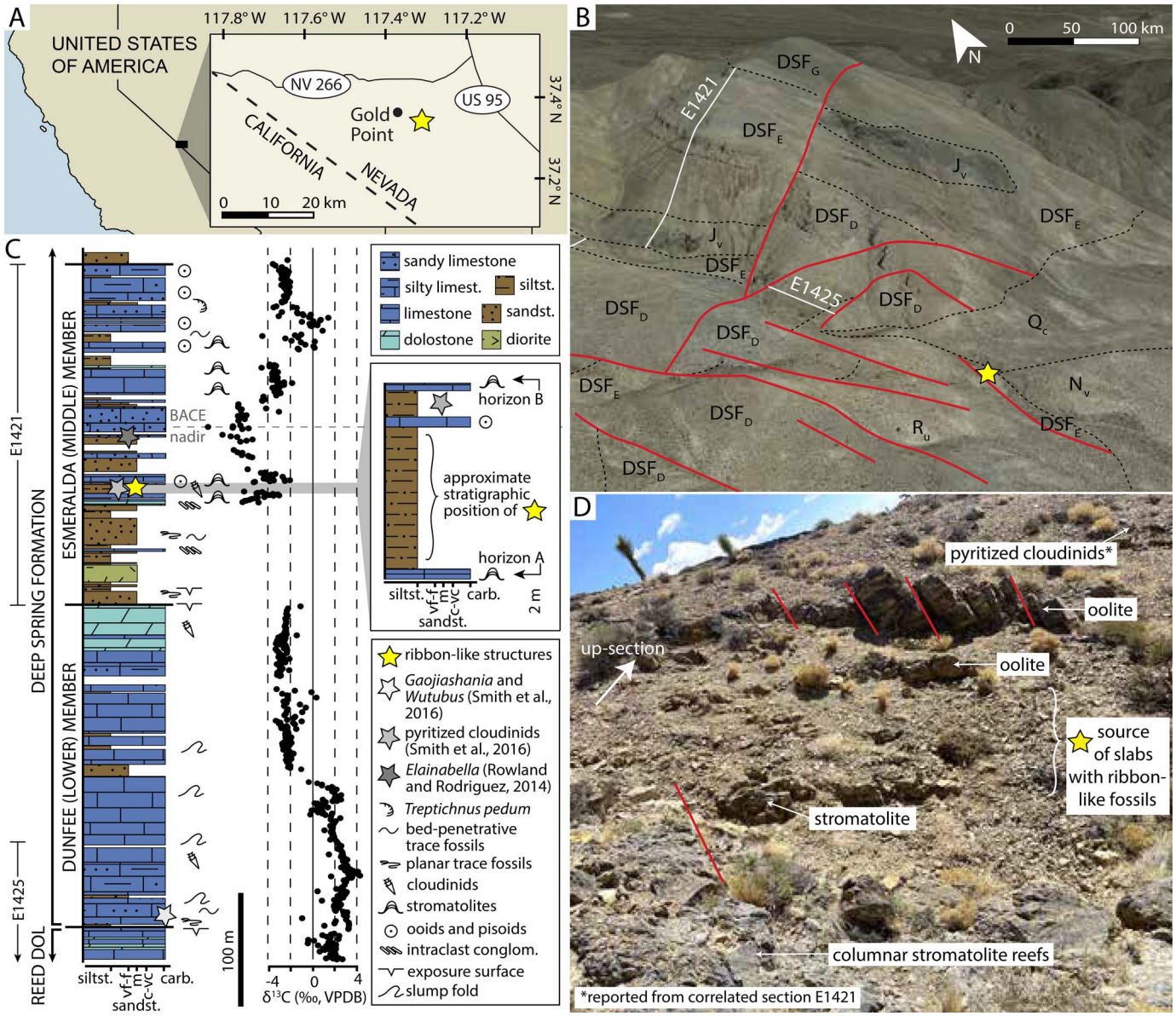

FIG. 1.—Geospatial and stratigraphic context of the ribbon-like structure reported from the Esmeralda Member of the Deep Spring Formation at Mount Dunfee. **A**) Locality map. Yellow star = Mount Dunfee/the sample site. **B**) Geologic contacts mapped onto a topographic projection of Google satellite imagery of Mount Dunfee, after the geologic map of Smith et al. (2016). Symbols: yellow star = sample site; white lines = previously published stratigraphic sections from which body fossil assemblages are reported (Smith et al. 2016); red lines = faults; black dashed lines = depositional and intrusive contacts. Geologic unit labels: R_u = upper member of the Reed Dolostone; DSF_D = Dunfee Member of the Deep Spring Formation; DSF_E = Esmeralda Member of the Deep Spring Formation; J_v = Jurassic volcanics; N_v = Neogene volcanics; Q_c = Quaternary cover. **C**) Litho-, chemo-, and biostratigraphy of the Dunfee and Esmeralda members of the Deep Spring Formation at Mount Dunfee. Stratigraphic data from the Dunfee and Esmeralda members of the Deep Spring Formation are displayed at ~ 2 m resolution after Smith et al. (2016). Additionally, a ~ 10 m-thick fossiliferous stratigraphic interval of the Esmeralda Member is displayed at ~ 0.2 m resolution. Abbreviations: limest. = limestone; siltst. = siltstone; sandst. = sandstone. **D**) Annotated outcrop photo of a hill adjacent to the gully from which samples were collected. Red lines = faults; yellow star = sample site.

characterization of late Ediacaran communities and report a new assemblage of smooth-walled, ribbon-like putative macroalgal fossils preserved as compressed casts and molds within siltstones of the Esmeralda Member of the Deep Spring Formation in Nevada, USA.

GEOLOGIC BACKGROUND

The southern Great Basin is oddly depauperate of Ediacaran body fossils, given the amount of low-grade and well-exposed Ediacaran strata preserved within it relative to other regions globally (Evans et al. 2024). Reports of Ediacaran body fossil occurrences in the region are largely restricted to specific sites and/or stratigraphic sections (Smith et al. 2023). One site in the southern Great Basin that has yielded three Ediacaran body fossil horizons with soft body preservation is near Mount Dunfee, Nevada, ~ 4 km to the southeast of the townsite of Gold Point (Fig. 1). These horizons occur within the Deep Spring Formation, a ~ 460 m-thick mixed siliciclastic and carbonate succession that is interpreted to record deposition within a slope to shelf setting and is divided into the Dunfee (lower), Esmeralda (middle), and Gold Point (upper) members (Stewart 1970; Gevirtzman and Mount 1986; Rowland et al. 2008; Ahn et al. 2012; Smith et al. 2023; Fig. 1C). All these

fossiliferous horizons with soft body preservation occur below the local placement of the Ediacaran–Cambrian boundary, which is marked by the local first occurrence of *Treptichnus pedum* (Corsetti and Hagadorn 2003) and the basal Cambrian negative carbon isotope excursion (BACE; Corsetti and Kaufman 1994; Smith et al. 2016).

The lowermost of these Ediacaran fossil horizons with soft body preservation occurs at the base of the Dunfee Member and has yielded casts and molds of *Gaojiashania* and *Wutubus*, compressions of putative algal fossils, and lightly pyritized compressed smooth-walled problematic tubular fossils (Smith et al. 2016; Rivas et al. 2024). The second horizon also preserves a tubular fossil assemblage. It occurs within the Esmeralda Member, ~ 100 m above the Dunfee-Esmeralda contact, and consists of pyritized cloudinomorphs (*Conotubus* and *Saarina*; Smith et al. 2016; Selly et al. 2020). Lastly, in the third and uppermost horizon, a single specimen of a kerogenized problematic branching algal fossil (*Elainabella deepspringensis*) is reported from a horizon ~ 150 m above the base of the Esmeralda Member (Rowland and Rodriguez 2014). However, unpublished scanning electron microscopic (SEM) analyses suggest that the syngenicity of this fossil may need to be further explored (J. Schiffbauer personal communication 2024).

Trace fossils other than *Treptichnus pedum* are also reported from the Deep Spring Formation at Mount Dunfee (Gevirtzman and Mount 1986; Smith et al. 2016; Tarhan et al. 2020; Fig. 1C). At the base of the Dunfee Member, within the same few meters of strata from which tubular body fossils are reported, mm-scale bed-planar trace fossils occur. They include furrows, identified as *Helminthoidichnites*, *Helminthopsis*, and *Cochlichnus*, infilled simple burrows, identified as *Planolites*, sinusoidal burrows that resemble *Belorhaphe*, and spiraling burrows that resemble *Helicolithus* (Gevirtzman and Mount 1986; Tarhan et al. 2020). Sub-horizontal plug-type traces resembling *Bergaueria* and simple treptichnid structures are also reported from this interval (Gevirtzman and Mount 1986; Tarhan et al. 2020). Bed-planar trace fossils are again reported at and ~ 50 m above the Dunfee-Esmeralda contact (Smith et al. 2016). All these trace fossils are similar to other latest Ediacaran trace fossil assemblages globally (e.g., Darroch et al. 2021).

The Mount Dunfee area has been extensively deformed by Cenozoic brittle deformation manifested as high-angle strike-slip and normal faults (Stewart 1970; Albers and Stewart 1972; Smith et al. 2016; Fig. 1B). Despite the structural complexity of the area, several marker beds within the Deep Spring Formation, especially the Esmeralda Member, allow for precise correlation between fault blocks and thus precise stratigraphic placement of fossil horizons, even when they occur within small, isolated fault blocks. Specifically, within the Esmeralda Member, distinctive microbial horizons (designated A–E), brown to black shale-siltstone intervals, oolitic grainstone beds, and sandy grainstone beds facilitate the regional correlation of stratigraphic intervals (Stewart 1970; Oliver and Rowland 2002; Rowland et al. 2008; Smith et al. 2016; Fig. 1C). The pyritized cloudinid assemblage reported from the Mount Dunfee area occurs within a brown to black siltstone-shale interval that directly overlies an oolitic lime grainstone that occurs between microbial horizons B and C (Smith et al. 2016).

METHODS

Fossils were collected from a fault block of the Esmeralda Member of the Deep Spring Formation, in a gully located ~ 1 km to the southeast of the peak of Mount Dunfee (N37.339901°, W117.319250°; Fig. 1B–1D). Twelve 6–32 cm^2 slabs of tan-green siltstone were collected from a talus slope on the side of a small gully, yielding > 200 fossils in total (Fig. 2A). Recessive beds of the same tan-green siltstone outcrop poorly < 10 m up a small ridge adjacent to the gully (Fig. 1C, 1D). Fossil specimens were imaged at Johns Hopkins University (JHU) using a Canon Rebel T3 DSLR camera with a 28–135 mm lens and a Leica M125 Stereo Microscope with a DFC550 digital camera. Fossil lengths and widths were measured using the measure tool on Adobe Illustrator. Collected fossil-bearing slabs are reposited at the Smithsonian Institution National Museum of Natural History (USNM) (samples PAL 799769 and PAL 799770).

Two specimens were isolated from the fossiliferous slabs using a diamond blade tile saw. These specimens were then carbon coated, imaged by SEM in backscattered electron (BSE) mode, and analyzed by energy dispersive electron spectroscopy (EDS) at the JHU Materials Characterization and Processing Facility (MCP). EDS analyses of 11 points within a single specimen, six on the fossil surface and five on the surrounding matrix, were completed using a Thermo Fisher Helios G4 UC Focused Ion Beam SEM with an EDAX Elite Silicon Drift Detector. Point analyses targeted flat areas to reduce biases associated with topographic variation (e.g., Meyer et al. 2012). They were completed using an accelerating voltage of 15 kV and a working distance of ~ 10 mm. An elemental map of a portion of the other prepared specimen was produced under the same operating conditions.

Portions of the fossil infilling were scraped off with a dental tool and applied to ultra-thin carbon Transmission Electron Microscope (TEM) grids and examined in a JEOL F200 TEM at the MCP. Conventional TEM, selected area diffraction patterns (SAED) and EDS spectra were collected on grains found in the scrapings.

RESULTS

Stratigraphic Occurrence

The analyzed siltstone samples contain distinctive ribbon-like structures visible in hand sample (Fig. 2A). The samples, which were collected from float, are interpreted to have been sourced from *in-situ* poorly outcropping siltstone-shale beds that occur lateral to the sampled site, based on physical proximity and shared lithology (Fig. 1B, 1D). The identification of marker beds stratigraphically above and below this *in-situ* siltstone-shale interval allowed for the approximate lithostratigraphic correlation (within < 5 m) of collected slabs with strata from a continuous, published stratigraphic section of the Esmeralda Member (Smith et al. 2016, section E1421) approximately 200 m northwest of our sample site (Fig. 1B). The siltstone-shale beds occur stratigraphically above a columnar stromatolite horizon identified as microbial horizon B from Rowland et al. (2008) and below a lime ooid grainstone marker bed. They are, therefore, suggested to correlate to strata ~ 2–10 m below the dark shale horizon from which pyritized cloudinids are reported (Smith et al. 2016; Selly et al. 2020; Fig. 1C, 1D). This lithostratigraphic correlation suggests that the newly reported fossil horizon occurs ~ 115 m below the first local occurrence of *T. pedum* and ~ 50 m below the BACE (Fig. 1C), indicating that the fossils are latest Ediacaran in age (< 538.8 Ma; Peng et al 2020). Chemo- and biostratigraphic integration of section E1421 into a regional age model by Nelson et al. (2023) suggests the newly reported fossils could be as young as ~ 533 Ma. Additional nearby fault blocks, including the fault block with section E1421 from Smith et al. (2016), were searched as part of this study, but no additional ribbon-like tubular fossils were found.

Description of Specimens

The structures preserved within the collected samples are macroscopic, randomly oriented, straight to gently curved, and ribbon-like (Fig. 2). They are typically orange to reddish-brown and sometimes have darker red-brown edges (Fig. 2). They lack striations or similar markings in hand-sample and SEM-BSE images (Figs. 2, 3). From the > 200 ribbon-like fossils, a subset of 50 was measured to have a width range of 0.22 mm to 0.74 mm (average of 0.45 mm), with 90% of fossils measured to be > 0.33 mm-wide and < 0.59 mm-wide (Online Supplemental File Table S1). Width variation within individual specimens was also observed. When significant (> 0.2 mm) variation in width occurs within a single specimen, it is caused by pinching, folding, and/or twisting of the specimen wall (Fig. 2B, 2C, 2E). Non-uniform bending is observed from several specimens (e.g., Fig. 2B, 2C), indicating

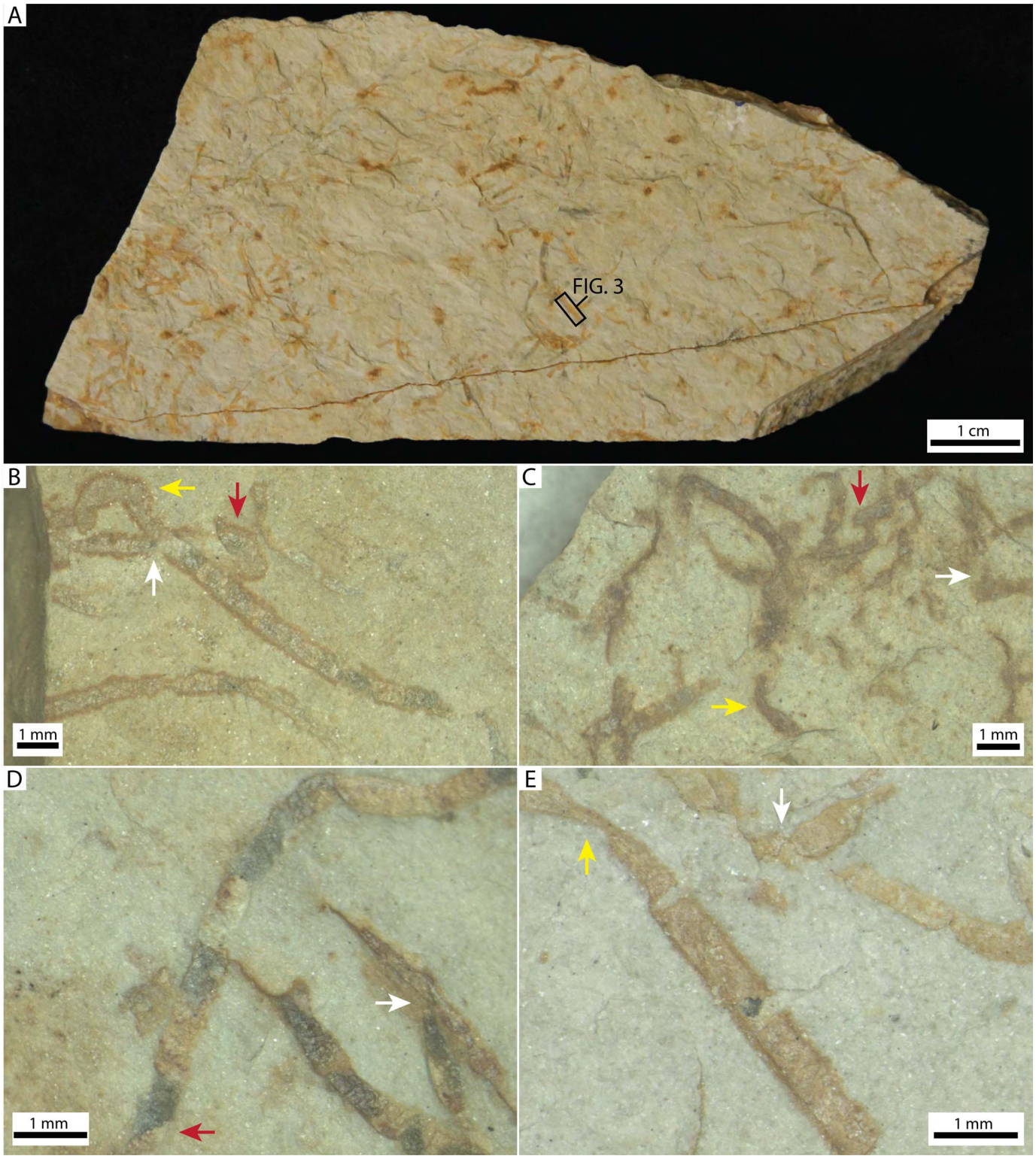

FIG. 2.—Photographs and photomicrographs of specimens from the Esmeralda Member of the Deep Spring Formation at Mount Dunfee. **A**) Photograph of a sample USNM-PAL-799769 with multiple ribbon-like compressions on surface. Boxed area = extent of BSE image in Figure 3. **B–E**) Photomicrographs of sample USNM-PAL-799770 specimens displaying possible branching or overlap (white arrows), pinching associated with bending (yellow arrows), and angular termination (red arrows).

that the walls were originally flexible. Several of the fossils do not have clear terminations and instead appear to laterally fade into the surrounding matrix, indicating bending out of the surface plane of the sample (Fig. 2). Other fossils have angular terminations (Fig. 2B–2D), implying the fossils are fragmented. As a result, true lengths are difficult to measure. However, the longest specimen measured has a length of ~ 7.5 mm, and the smallest has a length of ~ 1 mm. The density of ribbon structures on a slab surface varies significantly within and between slabs, with one slab containing areas with

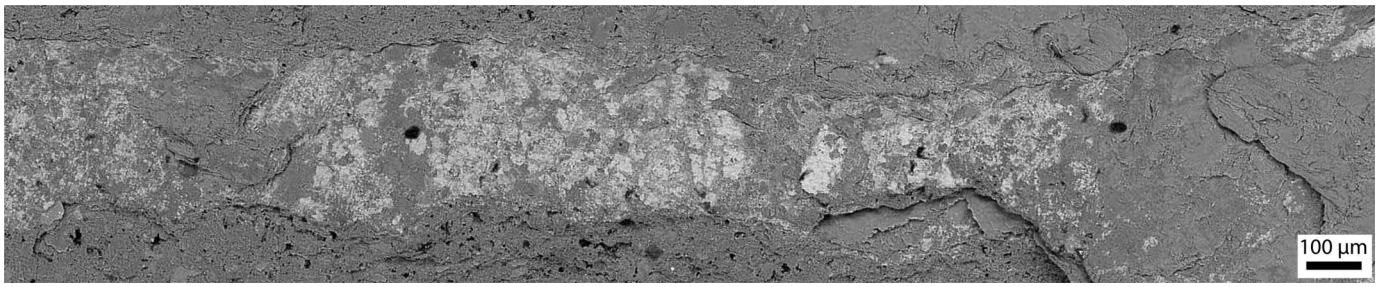

FIG. 3.—BSE image mosaic of sample USNM-PAL-799769 capturing a ribbon-like specimen (light-colored regions) and surrounding matrix (dark-colored regions). The BSE image extent spans the boxed area of Figure 2A.

$>$ 10 ribbons/cm^2 and others containing $<$ 1/cm^2. In areas with abundant ribbon structures, the structures sometimes overlap with each other (Fig. 2C). Possible branching is noted in some specimens (Fig. 2B–2E) but cannot be confidently distinguished from the overlapping of specimens.

Elemental Compositions of Fossils and the Surrounding Matrix

BSE imaging and EDS elemental mapping indicate that fossils are compositionally distinct from the matrix. BSE images reveal that the matrix is composed of a variety of platy and irregular minerals that are typically $<$ 20 µm across and uniformly gray-toned (Fig. 3). EDS point spectra and maps demonstrate that this material is composed of Si, Al, Mg, K, Ca, O, and minor Fe (Figs. 4, 5, Online Supplemental File Fig. S1; Online Supplemental File Table S2). In contrast, fossils stand out in BSE images as lighter gray or white, indicating that the fossil material is composed of heavier elements compared to the surrounding matrix (Fig. 3). EDS elemental mapping supports this characterization of the fossil composition; EDS maps and point spectra indicate that, like the matrix, the fossils contain Si, Al, Mg, and variable amounts of Ca, K, and Fe (Figs. 4, 5, Online Supplemental File Fig. S2; Online Supplemental File Table S2), but are enriched in Fe and depleted in Si relative to the matrix. Additionally, EDS point spectra from individual points within the fossils and scrapings from the fossils indicate compositional variability. Specifically, the Fe:Si ratio is variable within a given fossil, with some spots showing Fe:Si ratios $>$ 5 and others showing Fe:Si ratios $<$ 5 (Figs. 5, Online Supplemental File Figs. S2, S3; Online Supplemental File Table S2). Conventional TEM images, SAED patterns, and EDS spectra of scrapings from the fossil region suggest there are three distinct mineral phases within the fossils: an acicular mineral that, relative to the other minerals present, is Si-poor (Online Supplemental File Fig. S3A–S3D) and two platy minerals, one of which is Fe-poor relative to the other minerals present (Online Supplemental File Fig. S3E, S3F).

DISCUSSION

Taxonomy

Ribbon-like structures previously reported from Ediacaran strata include body fossils (e.g., Bykova et al. 2020), trace fossils (e.g., Jensen 2003), and pseudofossils (e.g., Petrov and Vorob'eva 2023). The compilation of some of the defining features of the structures reported here—their random orientations, variable densities, and occasional curvatures (Fig. 2)—is inconsistent with the latter interpretation. While individually, these features are not necessarily diagnostic of biogenicity, collectively, they are inconsistent with synsedimentary or diagenetic structures known to occur in siltstones and shales like mudcracks, debris flow clasts, and soft-sediment deformation structures. Instead, they are characteristics of many trace fossils and tubiform and ribbon-like body fossils from the Ediacaran Period, which are typically randomly oriented and distributed as a function of random movement or clustering of organisms within the sediment (e.g., Hofmann 1994; Jensen 2003).

Although the collection of features described here allows confident interpretation of a biogenic origin for these structures, further characterization of the assemblage is complicated by similarities shared between ribbon-like body fossil compressions and sinuous bed-planar trace fossils. Both sub-planar traces and ribbon-like body fossils are relatively common in terminal Ediacaran strata globally (e.g., Hofmann 1994; Jensen 2003), although, of them, only traces have been confidently identified from the Deep Spring Formation (Tarhan et al. 2020). Because of their simple, similar morphologies, these fossil types are commonly confused for each other in the field (e.g., Jensen 2003; Jensen et al. 2005). They also cannot be distinguished easily on a taphonomic basis; burrowing activity and diagenesis can result in compositional differences between the fossil burrow and surrounding matrix, while organic matter degradation during diagenesis can result in the absence of organic matter from body fossils and trace fossils (Jensen et al. 2005). Despite these difficulties, we interpret the newly reported structures as body fossils. This interpretation is based on: (1) observed width changes associated with fossil bending/original flexibility (Fig. 2B, 2C) and (2) angular terminations indicative of possible fossil fragmentation (Fig. 2B–2E). These characteristics are not shared with trace fossils, including those reported from the Esmeralda Member at Mount Dunfee (Jensen et al. 2005; Tarhan et al. 2020).

Given this interpretation and the morphology of these fossils, we suggest that they are likely members of the problematicum *Vendotaenia*. Vendotaenids were first described in detail by Gnilovskaya (1971) from Ediacaran strata of the East European Platform but have since been reported from Neoproterozoic and Cambrian successions globally (e.g., Sokolov 1975; Vidal 1981; Steiner 1994; Vidal et al. 1994; Gaucher et al. 2003; Cohen et al. 2009; Högström et al. 2013; Dornbos et al. 2016; Li et al. 2020; Maloney et al. 2023). They are characteristically 0.25–3.5 mm-wide and feature tubiform or ribbon-like thalli, rare branching, and longitudinal striations (Gnilovskaya 1971, 1983, 1985; Gnilovskaya et al. 1988). Our suggested classification is thus based on the range of the fossil widths measured (0.22 mm to 0.74 mm; Online Supplemental File Table S1) as well as the surface features, like the presence of defined edges and lack of internal striations (Online Supplemental File Fig. 2E), commonly observed from them. It is also consistent with the observation of possible branching (Gnilovskaya 1983; Cohen et al. 2009).

There are other late Ediacaran tubular body fossils described in the literature. These include *Sinocylindra yunnanensis* from the upper Doushantuo Formation in South China (Chen and Erdtmann 1991; Xiao et al. 2002; Yuan et al. 2002; Ye et al. 2019) and *Jiuqunaoella simplicis* from the Khatyspyt Formation of northern Siberia (Grazhdankin et al. 2008), Lyamtsa Formation of the East European Platform (Grazhdankin et al. 2007), and upper Doushantuo Formation in South China (Chen and Xiao 1991; Xiao et al. 2002; Ye et al. 2019). These ribbon-like fossils are similar in age (i.e., latest Ediacaran) and morphology to those reported here from Mount Dunfee, and have size ranges that overlap with, but do not

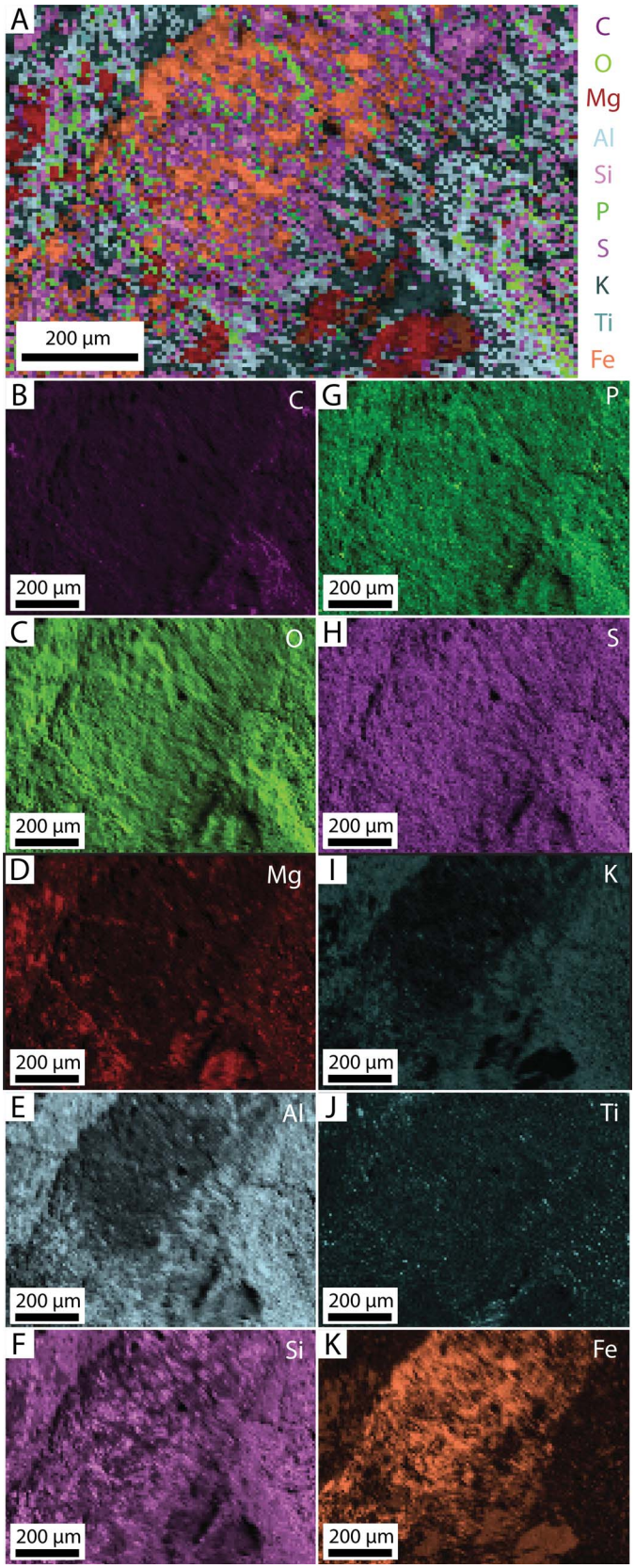

FIG. 4.—EDS elemental maps for sample USNM-PAL-799769 showing the distribution of C, O, Mg, Al, Si, P, S, K, Ti, and Fe. **A**) All element maps. **B–K**) Individual maps. White bar = 200 µm.

encompass, that observed for the Mount Dunfee specimens (Xiao et al. 2002; Ye et al. 2019). However, these fossils demonstrate some key features that are different from the fossils described here: *S. yunnanensis* displays constant widths, *J. simplicis* displays transverse wrinkles, and both taxa are unbranched (Xiao et al. 2002). We therefore consider the fossils described here to be taxonomically distinct from *S. yunnanensis* and *J. simplicis*. Instead, we favor an interpretation of these structures as vendotaenids, providing the first evidence of this group of fossils from the southern Great Basin.

Taphonomy

Crystal morphologies, EDS spectra, and relative weight percentages, while qualitative, suggest that the vendotaenid fossils at Mount Dunfee are likely composed of a combination of an Fe-oxide and possible Fe-rich aluminosilicate clays, preserved within an aluminosilicate matrix (Figs. 5, Online Supplemental File Fig. S3, Online Supplemental File Table S2). SAED patterns indicate the Fe-oxide is likely hematite (Online Supplemental File Fig. S3A). The composition and heterogeneity of the mineral assemblage interpreted to comprise the fossils implies that the fossils were not originally mineralized. We therefore instead suggest that the fossils were once organic-walled, despite being no longer carbonaceous (Figs. 4B, 5). This interpretation is consistent with the characterization of the fossils as originally flexible.

The timing of organic wall decomposition is not well-constrained, largely because the mechanism behind it is unclear. The host rocks that preserve the vendotaenid assemblage are of greenschist metamorphic grade, implying that once-present organic material may have been lost due to regional metamorphism. In such a scenario, organic walls may have been preserved during early diagenesis but were lost through later stages of diagenesis and metamorphism. Alternatively, the organic matter may have been degraded and lost during the earliest stages of diagenesis. If so, degradation must have been accompanied by early mineral forming processes to preserve the fossil. In such a scenario, the Fe-oxide phases that now preserve the vendotaenids described here could be alteration products of originally pyritized fossils.

Pyrite alteration would be consistent with other previously described Ediacaran vendotaenid assemblages. For example, in South China, the Dengying Formation contains vendotaenids preserved as carbonaceous compressions associated with sulfate derived from pyrite oxidation (Anderson et al. 2011), and in Namibia, the Feldschuhhorn Member of the Nama Group contains vendotaenids with walls that feature honeycomb-like textures, suggestive of the oxidative weathering of pyrite (Cohen et al. 2009). We do not observe Fe-S rich minerals or crystal morphologies indicative of pyrite preserved in the vendotaenid assemblage at Mount Dunfee today (e.g., Online Supplemental File Fig. S3B), but the iron-minerals that preserve the fossils may be oxidized products of originally pyritized fossils. The presence of pyritized cloudinids in siltstone ~ 2–8 m stratigraphically above the vendotaenid assemblage suggests that, at minimum, conditions suitable for pyrite precipitation existed relatively soon after vendotaenid deposition. These conditions include sediment pore waters with reduced iron, sulfate, sulfate-reducing microbes (SRM), and a carbon source (e.g., Schiffbauer et al. 2014, 2020). Variations on this taphonomic window have been described as "goldilocks scenarios" because any one of the necessary ingredients may become limiting and result in differences in the degree of pyrite formation and organic degradation (Schiffbauer et al. 2020). If the Fe-oxides that preserve the vendotaenid fossils at Mount Dunfee were pyrite alteration products, then the absence or low abundance of organic matter preserved in the fossils is consistent with the model that the availability of carbon was the limiting factor in preservation, resulting in near complete organic decay accompanying pyritization (Schiffbauer et al. 2020). This taphonomic model also implies a

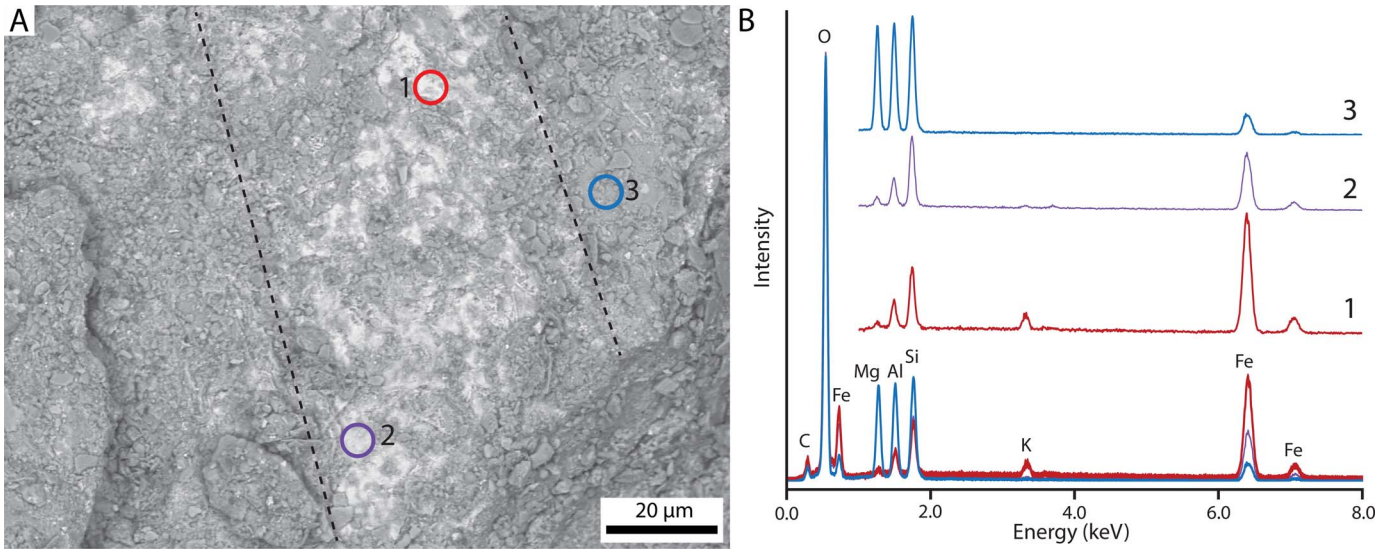

FIG. 5.—EDS points for sample USNM-PAL-799769 comparing the specimen surface (red and purple points) and surrounding matrix (blue point). **A**) Annotated BSE image with three annotated EDS point analysis locations. Annotations: dashed black line = approximate fossil bounds; red circle = point 1 (on fossil surface); purple circle = point 2 (on fossil surface); blue circle = point 3 (on matrix). **B**) EDS spectra from three points, displayed together and separately. Spectra taken at 15 keV. The red and purple lines represent the ribbon, while the blue line represents the surrounding matrix. All EDS analysis points produce peaks associated with C, O, Fe, Mg, Al, and Si. The specimen consistently shows elevated Fe and depleted Mg, Al, and Si relative to the matrix (red and purple v. blue points), but the degree of elevation/depletion varies spatially (red v. purple points).

low abundance of organic carbon in the sediment, largely confining pyrite precipitation to the carcasses (Farrell et al. 2013; Farrell 2014).

The timing of the formation or adsorption of the possible Fe-rich clays interpreted from the analyzed fossil material is also unclear; these clays may represent the original mineralogy of clays that infilled and/or coated organic walls during deposition/early diagenesis (e.g., Cohen et al. 2009; Anderson et al. 2011) or may be the result of late-stage alteration (e.g., Becker-Kerber et al. 2022). Because the fossiliferous strata are of greenschist facies, the origin of these possible clays cannot be resolved, but their composition is consistent with preservation mechanisms of other fossils described at Mount Dunfee (e.g., Rivas et al. 2024). The formation of authigenic Fe-rich clays has recently been suggested to have played a critical role in the moldic preservation of the *Gaojiashania* fossils that are reported at Mount Dunfee, ~ 400 m below the vendotaenid assemblage described here (Rivas et al. 2024). In the taphonomic model proposed for these fossils, pore fluid conditions necessary for Fe-rich clay authigenesis are facilitated by seawater chemistry, specifically a high availability of dissolved silica and ferrous iron due to local and global geochemical cycling (Rivas et al. 2024). If this model is correct, these conditions likely persisted during deposition of the Esmeralda Member, providing a reasonable pathway for the syndepositional formation of Fe-rich clays that may be associated with the vendotaenid assemblage reported here.

Biostratigraphic and Paleoecological Significance

The identification of a vendotaenid fossil assemblage within the Esmeralda Member at Mount Dunfee establishes the presence of vendotaenids along the southwestern margin of Laurentia at the close of the Ediacaran Period. Because the fossils are randomly oriented and variably abundant between slabs, they appear to have experienced little transport post-mortem. They are therefore suggested to have lived within the shelf environment previously interpreted from the strata in which they are preserved by Rowland et al. (2008).

Vendotaenids have been reported from similar Ediacaran shallow marine successions globally, including from Gondwana (Brazil, Namibia, South Africa, South China, Spain, and Uruguay; e.g., Steiner 1994; Vidal et al. 1994; Gaucher et al. 2003; Cohen et al. 2009; Shen et al. 2009; Simón 2018; Ye et al. 2019; Amorim et al. 2020; Xiao et al. 2021), Baltica and Siberia (Belarus, Estonia, Moldova, Norway, Poland, Russia, and Ukraine; Gnilovskaya 1971, 1985, 1988; Sokolov 1975; Moczydlowska 1995, 2008; Kochnev and Karlova 2010; Högström et al. 2013; Golubkova et al. 2022), Mongolia (Dornbos et al. 2016), and Laurentia (Narbonne and Hofmann 1987). Problematica suggested to be either vendotaenids or trace fossils are also reported from siltstones from the upper Miette Group of northwestern Canada, putatively placing vendotaenids on the Laurentian continent during the late Ediacaran Period (Hofmann and Mountjoy 2010; van Wieren et al. 2024). The description of the vendotaenid assemblage at Mount Dunfee affirms the global distribution of vendotaenids in the late Ediacaran, as it establishes their presence in southwestern Laurentia.

Although considered problematic fossils, vendotaenids are widely argued to be macroalgae given their size, general morphology, and interpreted preservation of cell walls and oogonia (Gnilovskaya 1983, Cohen et al. 2009). More specifically, vendotaenids recently were interpreted as green or red algae in part because red and green algal body fossils are reported from strata as old as the terminal Mesoproterozoic, while brown algae are not thought to emerge until the Ordovician (Maloney et al. 2023; Choi et al. 2024). Studies that have characterized morphological and ecological evolutionary patterns of noncalcified macroalgae during the Proterozoic and early Paleozoic have broadly shown that there are increases in thallus size, morphospace range, and ecological complexity through time (Xiao and Dong 2006; Bykova et al. 2020). However, analysis of time-binned Ediacaran macroalgae shows drops in the same metrics in the terminal Ediacaran (~ 550–539 Ma), suggesting that the proposed extinction event c. 550 Ma affected both the Ediacara biota and macroalgae (Bykova et al. 2020). The data presented here from the Mount Dunfee vendotaenids are consistent with the previously published macroalgal trends, and the size and morphology of the reported fossils are consistent with the interpretation of low morphological disparity and little size variation in the terminal Ediacaran (Bykova et al. 2020).

The recognition of vendotaenids in the Deep Spring Formation and, putatively, the upper Miette Group implies unreported vendotaenids may be present in late Ediacaran siltstones deposited elsewhere along the

western margin of Laurentia. Broadly correlative units that might host these fossils include the lower Wood Canyon Formation of the Death Valley region (Stewart 1970) the upper Blueflower, Algae, and/or Cut Thumb formations of northwestern Canada (Aitken 1989; McMechan 2015; Moynihan et al. 2019), and the lower La Ciénega Formation of Sonora, Mexico (Stewart et al. 1984). However, the lack of reports of vendotaenids from these strata—particularly the relatively well-studied Wood Canyon (e.g., Hagadorn et al. 2000; Hagadorn and Waggoner 2000; Smith et al. 2017) and upper Blueflower formations (e.g., Hofmann et al. 1983; Narbonne and Aitken 1990; Narbonne 1994; Carbone et al. 2015; Boag et al. 2024)—implies that few vendotaenid assemblages are preserved in the late Ediacaran strata of western Laurentia. Consistent with this suggestion, vendotaenids from the upper Miette Group (Hofmann and Mountjoy 2010) and Esmeralda Member of the Deep Spring Formation (this study) are reported from only four and 12 slabs, respectively, and only nine vendotaenid specimens are reported from the lower Blueflower Formation (Narbonne and Hofmann 1987; Pyle et al. 2004). In contrast, in other terminal Ediacaran successions globally, vendotaenids occur within multiple stratigraphic sections and at multiple horizons (e.g., Gnilovskaya 1988; Cohen et al. 2009; Dornbos et al. 2016; Simón 2018; Nelson et al. 2022; Petrov et al. 2024).

The apparent paucity of vendotaenids preserved in Ediacaran strata in western Laurentia may be a product of taphonomic bias associated with the metamorphic grade of host rocks. Globally, vendotaenids are widely reported from strata that are largely unmetamorphosed or have experienced sub-greenschist facies metamorphism (e.g., Moczydlowska 1995, 2008; Becker-Kerber et al. 2022; Petrov et al. 2024). However, a low preservation potential of vendotaenids does not explain the rarity of vendotaenid reports from largely unmetamorphosed late Ediacaran strata that also exist in western Laurentia. For example, vendotaenids are not reported from late Ediacaran siltstones in the Wernecke Mountains of northwestern Canada, which are described as only slightly metamorphosed (Pyle et al. 2004) and are host to bed-planar Ediacaran body and trace fossils (e.g., Narbonne and Hofmann 1987; Boag et al. 2024). Similarly, a low preservation potential of vendotaenids does not explain why vendotaenids are numerously reported from some late Ediacaran successions comprised of sub-greenschist facies rocks (e.g., the Tamengo Formation at the Sobramil locality, Brazil; Amorim et al. 2020; Becker-Kerber et al. 2022), but are unreported from others (e.g., the Blueflower Formation at the Sekwi Brook area, northwestern Canada; Gordey et al. 2011; Carbone et al. 2015).

Alternatively, the depauperate vendotaenid record in Laurentia may reflect spatially variability among late Ediacaran marine ecosystems and/or in the macroalgal response to global ecological change during the terminal Ediacaran Period. Further sampling of Ediacaran siltstones in western Laurentia is necessary to test these possibilities.

CONCLUSIONS

Thin (0.23–0.74 mm-wide), randomly oriented ribbon-like structures preserved within siltstones of the terminal Ediacaran Esmeralda Member of the Deep Spring Formation at Mount Dunfee display bending indicative of original flexibility and potential angular terminations indicative of fragmentation. On the basis of these characteristics, we argue the structures are vendotaenids preserved as compressed casts and molds. BSE imaging and EDS analyses further support their interpretation as fossils, revealing compositional differences between ribbon fillings and the surrounding matrix. From EDS spectra and associated relative weight percentages, we interpret the matrix to dominantly consist of aluminosilicates and the fossil filling to consist of a combination of Fe-rich silicates and Fe-oxides. This interpreted fossil composition is consistent with the compression, infilling, and, potentially, pyritization of an organic-walled tube during early diagenesis, a taphonomic model that has been previously proposed for other Ediacaran vendotaenid assemblages (e.g., Cohen et al. 2009).

Although vendotaenids are commonly reported from Ediacaran strata globally, the vendotaenid assemblage at Mount Dunfee represents the first described occurrence of vendotaenids within a late Ediacaran succession from southwestern Laurentia and the first described occurrence of vendotaenids within any strata from the southern Great Basin. The Mount Dunfee vendotaenids extend the paleogeographic range of latest Ediacaran algal fossils, and their morphology and size are consistent with the characterization that, globally, there was low algal morphological disparity in the terminal Ediacaran (Bykova et al. 2020). The newly reported vendotaenid assemblage thus contributes to our understanding of terminal Ediacaran algal records on regional and global scales.

ACKNOWLEDGMENTS

We thank the Smithsonian Institution National Museum of Natural History for assistance with specimen accession. EFS acknowledges the funding support of the American Philosophical Society Lewis and Clark Fund for Exploration and Field Research in Astrobiology, NSF-EAR-2021064, and Johns Hopkins University. MS thanks the Ingenuity Project for support. We thank reviewers Phoebe Cohen and an anonymous reviewer for their constructive comments.

SUPPLEMENTAL MATERIAL

Data are available from the PALAIOS Data Archive: https://www.sepm.org/supplemental-materials.

REFERENCES

Ahn, S.Y., Babcock, L.E., and Hollingsworth, J.S., 2012, Revised stratigraphic nomenclature for parts of the Ediacaran–Cambrian Series 2 succession in the southern Great Basin, USA: Memoirs of the Association of Australasian Palaeontologists, v. 42, p. 105–114.

Aires, T., Marbà, N., Cunha, R.L., Kendrick, G.A., Walker, D.I., Serrão, E.A., Duarte, C.M., and Arnaud-Haond, S., 2011, Evolutionary history of the seagrass genus *Posidonia*: Marine Ecology Progress Series, v. 421, p. 117–130.

Aitken, J.D., 1989, Uppermost Proterozoic formations in central Mackenzie Mountains, Northwest Territories: Geological Survey of Canada Bulletin, v. 368, p. 1–26.

Albers, J.P. and Stewart, J.H., 1972, Geology and mineral deposits of Esmeralda County, Nevada: Nevada Bureau of Mines and Geology Bulletin, v. 78, p. 1–79.

Amorim, K.B., Afonso, J.W.L., Leme, J. de M., Diniz, C.Q.C., Rivera, L.C.M., Gómez, Gutiérrez, J.C., Boggiani, P.C., and Trindade, R.I.F., 2020, Sedimentary facies, fossil distribution and depositional setting of the late Ediacaran Tamengo Formation (Brazil): Sedimentology, v. 67, p. 3422–3450.

Amthor, J.E., Grotzinger, J.P., Schröder, S., Bowring, S.A., Ramezani, J., Martin, M.W., and Matter, A., 2003, Extinction of *Cloudina* and *Namacalathus* at the Precambrian–Cambrian boundary in Oman: Geology, v. 31, p. 431–434.

Anderson, E.P., Schiffbauer, J.D., and Xiao, S., 2011, Taphonomic study of Ediacaran organic-walled fossils confirms the importance of clay minerals and pyrite in Burgess Shale-type preservation: Geology, v. 39, p. 643–646.

Becker-Kerber, B., Elmola, A.A., Zhuravlev, A., Gaucher, C., Simões, M., Prado, G., Vintaned, J.G., Fontaine, C., Lino, L., and Sanchez, D.F., 2022, Clay templates in Ediacaran vendotaeniaceans: implications for the taphonomy of carbonaceous fossils: GSA Bulletin, v. 134, p. 1334–1346.

Boag, T.H., Busch, J.F., Gooley, J.T., Strauss, J.V., and Sperling, E.A., 2024, Deep-water first occurrences of Ediacara biota prior to the Shuram carbon isotope excursion in the Wernecke Mountains, Yukon, Canada: Geobiology, v. 22, e12597.

Bowyer, F.T., Wood, R.A., and Yilales, M., 2024, Sea level controls on Ediacaran–Cambrian animal radiations: Science Advances, v. 10, eado6462.

Bykova, N., LoDuca, S.T., Ye, Q., Marusin, V., Grazhdankin, D., and Xiao, S., 2020, Seaweeds through time: morphological and ecological analysis of Proterozoic and early Paleozoic benthic macroalgae: Precambrian Research, v. 350, e105875.

Carbone, C.A., Narbonne, G.M., Macdonald, F.A., and Boag, T.H., 2015, New Ediacaran fossils from the uppermost Blueflower Formation, northwest Canada: disentangling biostratigraphy and paleoecology: Journal of Paleontology, v. 89, p. 281–291.

Chen, J. and Erdtmann, B.D., 1991, Lower Cambrian fossil lagerstätte from Chengjiang, Yunnan, China: insights for reconstructing early metazoan life, *in* A.M. Simonetta and S. Conway Morris (eds.), The Early Evolution of Metazoa and the Significance of Problematic Taxa: Cambridge University Press, Cambridge, p. 57–75.

Chen, M. and Xiao, Z., 1991, Discovery of the macrofossils in the upper Sinian Doushantuo Formation at Miaohe, eastern Yangtze Gorges: Chinese Journal of Geology, v. 26, p. 317–324.

Choi, S.-W., Graf, L., Choi, J.W., Jo, J., Boo, G.H., Kawai, H., Choi, C.G., Xiao, S., Knoll, A.H., and Andersen, R.A., 2024, Ordovician origin and subsequent diversification of the brown algae: Current Biology, v. 34, p. 740–754.

Christie, H., Norderhaug, K.M., and Fredriksen, S., 2009, Macrophytes as habitat for fauna: Marine Ecology Progress Series, v. 396, p. 221–233.

Cohen, P.A., Bradley, A., Knoll, A.H., Grotzinger, J.P., Jensen, S., Abelson, J., Hand, K., Love, G., Metz, J., and McLoughlin, N., 2009, Tubular compression fossils from the Ediacaran Nama group, Namibia: Journal of Paleontology, v. 83, p. 110–122.

Corsetti, F.A. and Hagadorn, J.W., 2003, The Precambrian–Cambrian transition in the southern Great Basin, USA: The Sedimentary Record, v. 1, p. 4–8.

Corsetti, F.A. and Kaufman, A.J., 1994, Chemostratigraphy of Neoproterozoic–Cambrian units, White-Inyo Region, eastern California and western Nevada: implications for global correlation and faunal distribution: PALAIOS, v. 9, p. 211–219.

Darroch, S.A., Cribb, A.T., Buatois, L.A., Germs, G.J., Kenchington, C.G., Smith, E.F., Mocke, H., O'Neil, G.R., Schiffbauer, J.D., and Maloney, K.M., 2021, The trace fossil record of the Nama Group, Namibia: exploring the terminal Ediacaran roots of the Cambrian explosion: Earth-Science Reviews, v. 212, e103435.

Darroch, S.A., Smith, E.F., Laflamme, M., and Erwin, D.H., 2018, Ediacaran extinction and Cambrian explosion: Trends in Ecology and Evolution, v. 33, p. 653–663.

Darroch, S.A., Smith, E.F., Nelson, L.L., Craffey, M., Schiffbauer, J.D., and Laflamme, M., 2023, Causes and consequences of end-Ediacaran extinction: an update: Cambridge Prisms: Extinction, v. 1, e15.

Darroch, S.A., Sperling, E.A., Boag, T.H., Racicot, R.A., Mason, S.J., Morgan, A.S., Tweedt, S., Myrow, P., Johnston, D.T., and Erwin, D.H., 2015, Biotic replacement and mass extinction of the Ediacara biota: Proceedings of the Royal Society B, Biological Sciences, v. 282, e20151003.

Dornbos, S.Q., Oji, T., Kanayama, A., and Gonchigdorj, S., 2016, A new Burgess Shale-type deposit from the Ediacaran of western Mongolia: Scientific Reports, v. 6, e23438.

Evans, S.D., Smith, E.F., Vayda, P., Nelson, L.L., and Xiao, S., 2024, The Ediacara Biota of the Wood Canyon formation: latest Precambrian macrofossils and sedimentary structures from the southern Great Basin: Global and Planetary Change, v. 241, e104547.

Evans, S.D., Tu, C., Rizzo, A., Surprenant, R.L., Boan, P.C., McCandless, H., Marshall, N., Xiao, S., and Droser, M.L., 2022, Environmental drivers of the first major animal extinction across the Ediacaran White Sea-Nama transition: Proceedings of the National Academy of Sciences, v. 119, e2207475119.

Farrell, U.C., 2014, Pyritization of soft tissues in the fossil record: an overview *in* M. Laflamme, J.D. Schiffbauer, and S.A.F. Darroch (eds.), Reading and Writing of the Fossil Record: Preservational Pathways to Exceptional Fossilization: The Paleontological Society Papers, v. 20, p. 35–57.

Farrell, U.C., Briggs, D.E.G., Hammarlund, E.U., Sperling, E.A., and Gaines, R.R., 2013, Paleoredox and pyritization of soft-bodied fossils in the Ordovician Frankfort Shale of New York: American Journal of Science, v. 313, p. 452–489.

Gaucher, C., Boggiani, P., Sprechmann, P., Sial, A., and Fairchild, T., 2003, Integrated correlation of the Vendian to Cambrian Arroyo del Soldado and Corumbá Groups (Uruguay and Brazil): palaeogeographic, palaeoclimatic and palaeobiologic implications: Precambrian Research, v. 120, p. 241–278.

Gevirtzman, D.A. and Mount, J.F., 1986, Paleoenvironments of an earliest Cambrian (Tommotian) shelly fauna in the southwestern Great Basin, USA: Journal of Sedimentary Research, v. 56, p. 412–421.

Gnilovskaya, M., 1971, The oldest aquatic plants of the Vendian of the Russian Platform: Paleontological Journal, v. 3, p. 372–378.

Gnilovskaya, M., 1983, Vendotaenids, *in* A. Urbanek and A.Y. Rozanov (eds.), Upper Precambrian and Cambrian Paleontology of the East European Platform: Publishing House Wydawnictwa Geologiczne, Warsaw, p. 46–56.

Gnilovskaya, M., 1985, Vendotaenids-Vendian Metaphyta, *in* B. Sokolov and A. Ivanovsky (eds.), Vendskaya Sistema 1: Akademiia Nauk SSSR, p. 117–129.

Gnilovskaya, M., Istchenko, A., Kolesniko, C., Korenchuk, L., and Udalstov, A., 1988, Vendotaenids of the East European Platform: Nauka, Leningrad, p. 1–143.

Golubkova, E.Y., Kuzmenkova, O., Laptsevich, A., Kushim, E., Vaskaboinikava, T., and Silivanov, M., 2022, Paleontological characteristics of the upper Vendian–lower Cambrian sediments in the section of the North Polotsk Borehole of the East European Platform, Belarus: Stratigraphy and Geological Correlation, v. 30, p. 457–474.

Gordey, S.P., Roots, C.F., Martel, E., MacDonald, J., Fallas, K.M., and MacNaughton, R.B., 2011, Bedrock Geology, Mount Eduni (106A), Northwest Territories: Geological Survey of Canada, Ottawa, Open-File 6594, scale 1:250,000.

Grazhdankin, D.V., Balthasar, U., Nagovitsin, K.E., and Kochnev, B.B., 2008, Carbonate-hosted Avalon-type fossils in arctic Siberia: Geology, v. 36, p. 803–806.

Grazhdankin, D., Nagovitsin, K., and Maslov, A., 2007, Late Vendian Miaohe-type ecological assemblage of the East European platform: Doklady Earth Sciences, v. 417, p. 1183–1187.

Hagadorn, J.W., Fedo, C.M., and Waggoner, B.M., 2000, Early Cambrian Ediacaran-type fossils from California: Journal of Paleontology, v. 74, p. 731–740.

Hagadorn, J.W. and Waggoner, B., 2000, Ediacaran fossils from the southwestern Great Basin, United States: Journal of Paleontology, v. 74, p. 349–359.

Han, T.-M. and Runnegar, B., 1992, Megascopic eukaryotic algae from the 2.1-billion-year-old Negaunee Iron-Formation, Michigan: Science, v. 257, p. 232–235.

Hodgin, E.B., Nelson, L.L., Wall, C.J., Barrón-Díaz, A.J., Webb, L.C., Schmitz, M.D., Fike, D.A., Hagadorn, J.W., and Smith, E.F., 2021, A link between rift-related volcanism and end-Ediacaran extinction? Integrated chemostratigraphy, biostratigraphy, and U-Pb geochronology from Sonora, Mexico: Geology, v. 49, p. 115–119.

Hofmann, H., 1994, Proterozoic carbonaceous compressions ("metaphytes" and "worms"), *in* S. Bengtson (ed.), Early Life on Earth: Columbia University Press, New York, p. 342–357.

Hofmann, H.J., Fritz, W.H., and Narbonne, G.M., 1983, Ediacaran (Precambrian) fossils from the Wernecke mountains, northwestern Canada: Science, v. 221, p. 455–457.

Hofmann, H.J. and Mountjoy, E.W., 2010, Ediacaran body and trace fossils in Miette Group (Windermere Supergroup) near Salient Mountain, British Columbia, Canada: Canadian Journal of Earth Sciences, v. 47, p. 1305–1325.

Högström, A., Jensen, S., Palacios, T., and Ebbestad, J.O.R., 2013, New information on the Ediacaran–Cambrian transition in the Vestertana Group, Finnmark, northern Norway, from trace fossils and organic-walled microfossils: Norsk Geologisk Tidsskrift, v. 93, p. 95–106.

Jensen, S., 2003, The Proterozoic and earliest Cambrian trace fossil record; patterns, problems and perspectives: Integrative and Comparative Biology, v. 43, p. 219–228.

Jensen, S., Droser, M.L., and Gehling, J.G., 2005, Trace fossil preservation and the early evolution of animals: Palaeogeography, Palaeoclimatology, Palaeoecology, v. 220, p. 19–29.

Kimura, H., Matsumoto, R., Kakuwa, Y., Hamdi, B., and Zibaseresht, H., 1997, The Vendian–Cambrian δ13C record, North Iran: evidence for overturning of the ocean before the Cambrian Explosion: Earth and Planetary Science Letters, v. 147, p. E1–E7.

Knoll, A.H. and Carroll, S.B., 1999, Early animal evolution: emerging views from comparative biology and geology: Science, v. 284, p. 2129–2137.

Kochnev, B. and Karlova, G., 2010, New data on biostratigraphy of the Vendian Nemakit-Daldynian stage in the southern Siberian platform: Stratigraphy and Geological Correlation, v. 18, p. 492–504.

Kumar, S., 1995, Megafossils from the Mesoproterozoic Rohtas Formation (the Vindhyan Supergroup), Katni area, central India: Precambrian Research, v. 72, p. 171–184.

Laflamme, M., Darroch, S.A., Tweedt, S.M., Peterson, K.J., and Erwin, D.H., 2013, The end of the Ediacara biota: extinction, biotic replacement, or Cheshire Cat?: Gondwana Research, v. 23, p. 558–573.

Levin, P.S., 1991, Effects of microhabitat on recruitment variation in a Gulf of Maine reef fish: Marine Ecology Progress Series, v. 75, p. 183–189.

Li, G., Chen, L., Pang, K., Zhou, G., Han, C., Yang, L., Lv, W., Wu, C., Wang, W., and Yang, F., 2020, An assemblage of macroscopic and diversified carbonaceous compression fossils from the Tonian Shiwangzhuang Formation in western Shandong, North China: Precambrian Research, v. 346, e105801.

LoDuca, S.T., Bykova, N., Wu, M., Xiao, S., and Zhao, Y., 2017, Seaweed morphology and ecology during the great animal diversification events of the early Paleozoic: a tale of two floras: Geobiology, v. 15, p. 588–616.

Maloney, K.M., Maverick, D.P., Schiffbauer, J.D., Halverson, G.P., Xiao, S., and Laflamme, M., 2023, Systematic paleontology of macroalgal fossils from the Tonian Mackenzie Mountains Supergroup: Journal of Paleontology, v. 97, p. 499–515.

McMechan, M.E., 2015, The Neoproterozoic succession of the central Rocky Mountains, Canada: Bulletin of Canadian Petroleum Geology, v. 63, p. 243–273.

Meyer, M., Schiffbauer, J.D., Xiao, S., Cai, Y., and Hua, H., 2012, Taphonomy of the upper Ediacaran enigmatic ribbonlike fossil *Shaanxilithes*: PALAIOS, v. 27, p. 354–372.

Moczydlowska, M., 1995, Neoproterozoic and Cambrian successions deposited on the East European Platform and Cadomian basement area in Poland: Studia Geophysica et Geodaetica, v. 39, p. 276–285.

Moczydlowska, M., 2008, New records of late Ediacaran microbiota from Poland: Precambrian Research, v. 167, p. 71–92.

Moynihan, D.P., Strauss, J.V., Nelson, L.L., and Padget, C.D., 2019, Upper Windermere Supergroup and the transition from rifting to continent-margin sedimentation, Nadaleen River area, northern Canadian Cordillera: GSA Bulletin, v. 131, p. 1673–1701.

Muscente, A., Bykova, N., Boag, T.H., Buatois, L.A., Mángano, M.G., Eleish, A., Prabhu, A., Pan, F., Meyer, M.B., and Schiffbauer, J.D., 2019, Ediacaran biozones identified with network analysis provide evidence for pulsed extinctions of early complex life: Nature Communications, v. 10, p. 911.

Narbonne, G.M., 1994, New Ediacaran fossils from the Mackenzie Mountains, northwestern Canada: Journal of Paleontology, v. 68, p. 411–416.

Narbonne, G.M. and Aitken, J.D., 1990, Ediacaran fossils from the Sekwi Brook area, Mackenzie mountains, northwestern Canada: Palaeontology, v. 33, p. 945–980.

Narbonne, G.M. and Hofmann, H.J., 1987, Ediacaran biota of the Wernecke Mountains, Yukon, Canada: Palaeontology, v. 30, p. 647–676.

Nelson, L.L., Crowley, J.L., Smith, E.F., Schwartz, D.M., Hodgin, E.B., and Schmitz, M.D., 2023, Cambrian explosion condensed: high-precision geochronology of the lower Wood Canyon Formation, Nevada: Proceedings of the National Academy of Sciences, v. 120, p. e2301478120.

Nelson, L.L., Ramezani, J., Almond, J.E., Darroch, S.A., Taylor, W.L., Brenner, D.C., Furey, R.P., Turner, M., and Smith, E.F., 2022, Pushing the boundary: a calibrated Ediacaran–Cambrian stratigraphic record from the Nama Group in northwestern Republic of South Africa: Earth and Planetary Science Letters, v. 580, e117396.

Oliver, L.K. and Rowland, S.M., 2002, Microbialite reefs at the close of the Proterozoic Eon: The Middle Member Deep Spring Formation at Mt. Dunfee, Nevada, *in* F.A. Corsetti (ed.), Proterozoic–Cambrian of the Great Basin and Beyond: Society for Sedimentary Geology Pacific Section Book, v. 93, p. 97–122.

Peng, S.C., Babcock, L.E., and Ahlberg, P., 2020, The Cambrian Period, *in* F.M. Gradstein, J.G. Ogg, M.D. Schmitz, and G.M. Ogg (eds.), The Geologic Timescale: Elsevier, p. 565–629.

Petrov, P.Y. and Vorob'eva, N.G., 2023, Fossils, pseudofossils and problematica from the Ura Formation: Ediacaran of the Patom Basin, Siberia: Precambrian Research, v. 397, e107188.

Petrov, P.Y., Vorob'eva, N., and Ragozina, A., 2024, New data on the upper Ediacaran microbiota of Zuun-Arts (Zavkhan terrane, western Mongolia): Paleontological Journal, v. 58, p. 371–384.

Pyle, L.J., Narbonne, G.M., James, N.P., Dalrymple, R.W., and Kaufman, A.J., 2004, Integrated Ediacaran chronostratigraphy, Wernecke Mountains, northwestern Canada: Precambrian Research, v. 132, p. 1–27.

Rivas, A., Myrow, P.M., Smith, E.F., Nelson, L.L, Briggs, D.E.G., and Tarhan, L.G., 2024, Morphology and preservation of Gaojiashania, an enigmatic tubular fossil from the upper Ediacaran Dunfee Member, Deep Spring Formation, Nevada, USA: PALAIOS, v. 39, p. 444–461.

Rowland, S.M., Oliver, L.K., and Hicks, M., 2008, Ediacaran and early Cambrian reefs of Esmeralda County, Nevada: non-congruent communities within congruent ecosystems across the Neoproterozoic–Paleozoic boundary, *in* E.M. Duebendorfer and E.I. Smith (eds.), Field Guide to Plutons, Volcanoes, Faults, Reefs, Dinosaurs, and Possible Glaciation in Selected Areas of Arizona, California, and Nevada: Geological Society of America, Field Guide 11, p. 83–100.

Rowland, S.M. and Rodriguez, M.G., 2014, A multicellular alga with exceptional preservation from the Ediacaran of Nevada: Journal of Paleontology, v. 88, p. 263–268.

Schiffbauer, J.D., Selly, T., Jacquet, S.M., Merz, R.A., Nelson, L.L., Strange, M.A., Cai, Y., and Smith, E.F., 2020, Discovery of bilaterian-type through-guts in cloudinomorphs from the terminal Ediacaran Period: Nature Communications, v. 11, p. 205.

Schiffbauer, J.D., Xiao, S., Cai, Y., Wallace, A.F., Hua, H., Huner, J., Xu, H., Peng, Y., and Kaufman, A.J., 2014, A unifying model for Neoproterozoic–Palaeozoic exceptional fossil preservation through pyritization and carbonaceous compression: Nature Communications, v. 5, p. 5754.

Selly, T., Schiffbauer, J.D., Jacquet, S.M., Smith, E.F., Nelson, L.L., Andreasen, B.D., Huntley, J.W., Strange, M.A., O'Neil, G.R., and Thater, C.A., 2020, A new cloudinid fossil assemblage from the terminal Ediacaran of Nevada, USA: Journal of Systematic Palaeontology, v. 18, p. 357–379.

Shen, B., Xiao, S., Zhou, C., and Yuan, X., 2009, *Yangtziramulus zhangi* new genus and species, a carbonate-hosted macrofossil from the Ediacaran Dengying Formation in the Yangtze Gorges area, South China: Journal of Paleontology, v. 83, p. 575–587.

Simón, J., 2018, A transitional Ediacaran–Cambrian biota in the Abenójar anticline (Iberian Massif, Spain): Estudios Geológicos, v. 74, e084.

Smith, E.F., Nelson, L.L., O'Connell, N., Eyster, A., and Lonsdale, M.C., 2023, The Ediacaran–Cambrian transition in the southern Great Basin, United States: GSA Bulletin, v. 135, p. 1393–1414.

Smith, E.F., Nelson, L., Strange, M., Eyster, A., Rowland, S., Schrag, D., and MacDonald, F., 2016, The end of the Ediacaran: two new exceptionally preserved body fossil assemblages from Mount Dunfee, Nevada, USA: Geology, v. 44, p. 911–914.

Smith, E., Nelson, L., Tweedt, S., Zeng, H., and Workman, J.B., 2017, A cosmopolitan late Ediacaran biotic assemblage: new fossils from Nevada and Namibia support a global biostratigraphic link: Proceedings of the Royal Society B, Biological Sciences, v. 284, e20170934.

Sokolov, B., 1975, On paleontological finds in pre-Usol'e sediments of the Irkutsk Amphitheater, *in* B.S. Sokolov and V.V. Khomentovsky (eds.), Analogues of the Vendian Complex in Siberia: Nauka, Moscow, p. 112–117.

Steiner, M., 1994, Die neoproterozoischen Megaalgen Südchinas: Berliner Geowissenschaftliche Abhandlungen, v. E15, p. 1–146.

Stewart, J.H., 1970, Upper Precambrian and lower Cambrian strata in the southern Great Basin, California and Nevada: US Geological Survey Professional Paper 620, 206 p.

Stewart, J.H., McMenamin, M.A., and Morales-Ramírez, J.M., 1984, Upper Proterozoic and Cambrian rocks in the Caborca region, Sonora, Mexico; hysical Stratigraphy, Biostratigraphy, Paleocurrent Studies, and Regional Relations: US Geological Survey Professional Paper 1309, 36 p.

Tarhan, L.G., Myrow, P.M., Smith, E.F., Nelson, L.L., and Sadler, P.M., 2020, Infaunal augurs of the Cambrian explosion: an Ediacaran trace fossil assemblage from Nevada, USA: Geobiology, v. 18, p. 486–496.

Van Wieren, C.S., Husson, J.M., and Dyer, B., 2024, Chemostratigraphy of the Ediacaran Old Fort Point Formation in the southern Canadian Cordillera: Precambrian Research, v. 411, e107525.

Vidal, G., 1981, Micropaleontology and biostratigraphy of the Upper Proterozoic and lower Cambrian sequence in East Finnmark, northern Norway: Norges Geologiske Undersokelse Bulletin, v. 362, p. 1–53.

Vidal, G., Palacios, T., Gámez-Vintaned, J.A., Balda, M.A.D., and Grant, S.W., 1994, Neoproterozoic–early Cambrian geology and palaeontology of Iberia: Geological Magazine, v. 131, p. 729–765.

Wood, R., Liu, A.G., Bowyer, F., Wilby, P.R., Dunn, F.S., Kenchington, C.G., Cuthill, J.F.H., Mitchell, E.G., and Penny, A., 2019, Integrated records of environmental change and evolution challenge the Cambrian Explosion: Nature Ecology and Evolution, v. 3, p. 528–538.

Xiao, S., Chen, Z., Pang, K., Zhou, C., and Yuan, X., 2021, The Shibantan Lagerstätte: insights into the Proterozoic–Phanerozoic transition: Journal of the Geological Society, v. 178, ejgs2020–135.

Xiao, S. and Dong, L., 2006, On the morphological and ecological history of Proterozoic macroalgae, *in* S. Xiao and A.J. Kaufman (eds.), Neoproterozoic Geobiology and Paleobiology: Springer, Dordrecht, p. 57–90.

Xiao, S., Yuan, X., Steiner, M., and Knoll, A.H., 2002, Macroscopic carbonaceous compressions in a terminal Proterozoic shale: a systematic reassessment of the Miaohe biota, South China: Journal of Paleontology, v. 76, p. 347–376.

Ye, Q., Tong, J., An, Z., Hu, J., Tian, L., Guan, K., and Xiao, S., 2019, A systematic description of new macrofossil material from the upper Ediacaran Miaohe Member in South China: Journal of Systematic Palaeontology, v. 17, p. 183–238.

Yuan, X., Xiao, S., Yin, L., Knoll, A., Zhou, C., and Mu, X., 2002, Doushantuo Fossils: Life on the Eve of Animal Radiation: University of Science and Technology of China Press, Hefei, China, 71 p.

Received 25 September 2024; accepted 21 March 2025.